Monthly Notices
of the
ROYAL ASTRONOMICAL SOCIETY

MNRAS **488,** 3231–3237 (2019)
Advance Access publication 2019 July 10

doi:10.1093/mnras/stz1893

Proper motions of the satellites of M31

Ben Hodkinson[1] and Jakub Scholtz[2]★

[1]*Physics Department, Durham University, Durham, DH1 3LE, UK*
[2]*IPPP, Durham University, Durham, DH1 3LE, UK*

Accepted 2019 July 8. Received 2019 July 2; in original form 2019 June 24

ABSTRACT

We predict the range of proper motions of 19 satellite galaxies of M31 that would rotationally stabilize the M31 plane of satellites consisting of 15–20 members as identified by Ibata et al. Our prediction is based purely on the current positions and line-of-sight velocities of these satellites and the assumption that the plane is not a transient feature. These predictions are therefore independent of the current debate about the formation history of this plane. We further comment on the feasibility of measuring these proper motions with future observations by the THEIA satellite mission as well as the currently planned observations by *HST* and *JWST*.

Key words: proper motions – local group.

1 INTRODUCTION

Ibata et al. (2013) reported the existence of a planar sub-group of 15 satellites of the M31 galaxy, although there was evidence of a planar structure in the M31 system in earlier studies by Metz, Kroupa & Jerjen (2007, 2009). Of the 15 in-plane satellites, 13 are co-rotating, which suggests, but does not show, this plane is a kinematically stable structure. Moreover, the small width of the plane, roughly 13 kpc, is a challenge to explain. As a result, it is a matter of active debate if this structure may be an indication of phenomena not predicted within standard ΛCDM cosmology (Zentner et al. 2005; Cautun et al. 2015; Ibata et al. 2015; Pawlowski 2018). In particular, Gillet et al. (2015) and Buck, Dutton & Macciò (2016) have argued that kinematically stable planes are less common than accidental alignments in the standard ΛCDM scenario. Therefore, the question of whether this plane is a truly stable structure has important consequences for our understanding of the ΛCDM model: finding proper motions consistent with kinematically stable plane would sharpen the tension between the ΛCDM model and the observations.

A similar plane of satellites has previously been observed in the Centaurus A system (Müller et al. 2018). Even the Milky Way has a plane of satellites (Kroupa, Theis & Boily 2005). Moreover the proper motions (PMs) of the satellites of MW for which data were not already available were predicted under the assumption that the MW plane is rotationally stabilized (Pawlowski & Kroupa 2013, 2014; Pawlowski, McGaugh & Jerjen 2015; Fritz et al. 2018).

In this paper, we carry out a similar analysis for the satellite members of the plane of M31 based on our current knowledge of the satellites' orbital parameters, which includes their full three-dimensional position and line-of-sight velocities (Conn et al. 2012; McConnachie 2012). At first glance, a permanent membership of an individual satellite in the plane can be reduced to the condition that the satellite's angular momentum is aligned with the normal to the plane. This fixes one of the components of proper motion. The remaining component determines the size of the angular momentum of the satellite and is limited by the condition that the satellite is on a bound orbit. As a result the constraints implied by the stability of the plane result in a finite range of allowed values of their proper motions.

In this paper, we identify the range of possible PMs for the 13 co-rotating satellites, 2 counter-rotating satellites, and 5 additional satellites that were also reported in Ibata et al. (2013) as being consistent with a stable plane. Our results are a prediction and provide a benchmark against which measurements of the PMs can be compared to determine whether the plane is indeed a stable structure or a temporary alignment of satellites of M31.

We do feel the need to re-iterate two points: first, the results of this work are independent of the debate about the nature of this plane: it could be a rare structure of the ΛCDM model or a manifestation of a deviation from the ΛCDM. As long as the M31 plane is a stable feature, our results remain valid. Secondly, whether the plane is kinematically stabilized or an accidental alignment only observable in the current era is not a dichotomy: the answer may be that a subset of satellites form a kinematically stable plane, while the rest of the satellites are aligned accidentally.

This paper is organized as follows: in Section 2, we discuss our methods for determining properties of the satellites' orbits. In Section 3, we define the constraints an orbit needs to satisfy in order to belong to the plane. In Section 4, we discuss our results and the experimental program needed to probe these results. We conclude in Section 5.

★ E-mail: jakubscholtz@gmail.com

Table 1. Data from McConnachie (2012) and Conn et al. (2012) for the satellites reported in Ibata et al. (2013) to plausibly lie in the planar structure. The heliocentric distances are given in kpc, with upper and lower errors. The heliocentric velocities are given as line-of-sight velocities relative to the Sun with upper and lower errors. The top section of this table contains presumed members of the M31 plane, while the lower section consists of satellites whose membership is debatable.

Name	RA	Dec.	D (kpc)	$v_{\rm los}$ (km s^{-1})
And I	00 45 39.8	38 02 28	727^{+18}_{-17}	$-376.3^{+2.2}_{-2.2}$
And III	00 35 33.8	36 29 52	723^{+18}_{-24}	$-344.3^{+1.7}_{-1.7}$
And IX	00 52 53.0	43 11 45	600^{+91}_{-23}	$-209.4^{+2.5}_{-2.5}$
And XI	00 46 20.0	33 48 05	763^{+29}_{-106}	$-419.6^{+4.4}_{-4.4}$
And XII	00 47 27.0	34 22 29	928^{+40}_{-136}	$-558.4^{+3.2}_{-3.2}$
And XIII	00 51 51.0	33 00 16	760^{+126}_{-154}	$-185.4^{+2.4}_{-2.4}$
And XIV	00 51 35.0	29 41 49	793^{+23}_{-179}	$-480.6^{+1.2}_{-1.2}$
And XVI	00 59 29.8	32 22 36	476^{+44}_{-29}	$-367.3^{+2.8}_{-2.8}$
And XVII	00 37 07.0	44 19 20	727^{+39}_{-25}	$-251.6^{+1.8}_{-2.0}$
And XXV	00 30 08.9	46 51 07	736^{+23}_{-69}	$-107.8^{+1.0}_{-1.0}$
And XXVI	00 23 45.6	47 54 58	754^{+218}_{-164}	$-261.6^{+3.0}_{-2.8}$
And XXVII	00 37 27.1	45 23 13	1255^{+42}_{-474}	$-539.6^{+4.7}_{-4.5}$
And XXX	00 36 34.9	49 38 48	681^{+32}_{-78}	$-139.8^{+6.0}_{-6.6}$
NGC 147	00 33 12.1	48 30 32	712^{+21}_{-19}	$-193.1^{+0.8}_{-0.8}$
NGC 185	00 38 58.0	48 20 15	620^{+19}_{-18}	$-203.8^{+1.1}_{-1.1}$
M32	00 42 41.8	40 51 55	805^{+82}_{-74}	$-199.0^{+6.0}_{-6.0}$
NGC 205	00 40 22.1	41 41 07	824^{+27}_{-26}	$-286.5^{+0.3}_{-0.3}$
IC 10	00 20 17.3	59 18 14	794^{+45}_{-43}	$-348.0^{+1.0}_{-1.0}$
LGS 3	01 03 55.0	48 20 15	769^{+25}_{-24}	$-203.8^{+1.1}_{-1.1}$
IC 1613	01 04 47.8	02 07 04	755^{+43}_{-41}	$-231.6^{+1.2}_{-1.2}$

2 METHOD

2.1 Positions and velocities of the M31 system

We use the data available in McConnachie (2012) and in Conn et al. (2012) as presented in Table 1. We take the velocity of M31 with respect to the Sun, according to McConnachie (2012) and van der Marel et al. (2019), to be

$$\begin{aligned} v_{\rm los,M31} &= -300 \pm 4\,{\rm km\,s^{-1}} \\ \mu_{\alpha*,\rm M31} &= +65 \pm 18\ \mu{\rm as\,yr^{-1}} \\ \mu_{\delta,\rm M31} &= -57 \pm 15\ \mu{\rm as\,yr^{-1}}. \end{aligned} \tag{1}$$

In this paper, we will adopt a Cartesian coordinate system, aligned with the standard Galactic coordinate system, but centred on M31.

2.2 Properties of the plane of M31 satellites

For our purposes, it is best to describe the plane by a unit normal vector $\hat{n}$ and the offset of the plane away from the origin (centre of M31) along $\hat{n}$, d. Although each individual satellite orbit is contained in a plane that also contains the origin (the satellites orbit around M31), it does not mean that the plane of satellites itself has to contain the origin unless all the orbits are exactly co-planar.

We choose $\hat{n}$ and d such that the sum of the squares of distances of the satellites from the plane is minimized. Note that we exclude M32, NGC 205, LGS 3, IC10, and IC1613 in this calculation, as their planar membership is debatable, and consider just the first 15 satellites in Table 1. Denoting the position vectors of satellites by $\boldsymbol{r_i}$, then the sum of the squares of the distances is given by

$$D^2 = \sum_{i=1}^{15} D_i^2 = \sum_{i=1}^{15} |\boldsymbol{r}_i \cdot \boldsymbol{n} + d|^2. \tag{2}$$

We minimize D, subject to the normalization constraint $|\boldsymbol{n}| = 1$. This yields the normal vector and plane offset:

$$\begin{aligned} \hat{\boldsymbol{n}} &= [0.887, 0.443, -0.132] \\ d &= -3.5 \pm 1.5\,{\rm kpc}, \end{aligned} \tag{3}$$

where the uncertainty bands come from sampling the heliocentric distances of M31 and all the satellites from Gaussians with widths given by the uncertainty bands in Table 1. We omit the uncertainty bands for the pole, because the pole of the plane $\hat{\boldsymbol{n}}$ only varies by 1° (68 per cent confidence interval) under the same sampling.

Given $\hat{\boldsymbol{n}}$ and d, we can also compute the thickness of the plane:

$$\sigma_{\rm d} = \frac{D}{\sqrt{15}} = 12.4 \pm 0.8\,{\rm kpc}, \tag{4}$$

where the uncertainty band comes from the same distance sampling as described above.

2.3 Determining satellite orbits

Each choice of proper motion ($\mu_{\alpha*}$, μ_δ) is equivalent to a different orbit. As we will see in Section 3, we are interested in three properties of each orbit: the maximum distance of the satellite from the plane in the next 10 periapses

$$d_{\rm max} = \max_t |\boldsymbol{r}(t) \cdot \hat{\boldsymbol{n}} + d|, \tag{5}$$

and the minimum and maximum distances of the satellite from the centre of M31 (also over the next 10 periapses)

$$r_{\rm min} = \min_t |\boldsymbol{r}(t)| \tag{6}$$

$$r_{\rm max} = \max_t |\boldsymbol{r}(t)|. \tag{7}$$

Here we should briefly mention our choice of integration time. A possible choice would be to set a fixed integration time of the order of the age of M31, and we believe that this is an acceptable choice. However, there are orbits, which are only accidentally aligned with the plane and stay aligned for up to a couple billion years.

An example of such an orbit would be a highly eccentric orbit such that the plane of this orbit is not aligned with the plane of M31, but the major axis of this orbit lies along the intersect of these two planes. Because orbits in the potential of an NFW halo are not closed, after the next periapsis the major axis of the orbit changes significantly and the orbit is no longer close to the plane. These orbits represent temporary alignments between the orbit and a plane unrelated to the orbit.

Since we are interested in finding orbits that are not temporarily aligned with the plane of satellites, we would like to avoid accepting these orbits. In order to remove them, we choose to integrate over a fixed number of periapses: we chose this fixed number to be 10.

For comparison with other work, we also compute the angle between the normal to the plane from equation (3) and the angular

momentum of the satellite $\boldsymbol{L} = \boldsymbol{r} \times \boldsymbol{v}$ around the centre of M31:

$$\cos\theta = \boldsymbol{L} \cdot \hat{\boldsymbol{n}}/|\boldsymbol{L}|. \quad (8)$$

In order to compute these quantities we use GALPOT (McMillan 2016) to integrate the orbits in the gravitational field of M31. We model M31 as re-scaled DM halo of the Milky Way. We use an NFW dark matter halo with density profile

$$\rho(r) = \frac{\rho_0}{(r/r_0)(1 + r/r_0)^2}, \quad (9)$$

where $\rho_0 = 1.7 \times 10^7\ \mathrm{M_\odot\,kpc^{-3}}$ (corresponds to $M_{\rm M31} \sim 2M_{\rm MW} \sim 2.6 \times 10^{12}\ \mathrm{M_\odot}$) and the scale radius $r_s = 19$ kpc (McMillan 2017). We have also produced results for a Milky Way like potential with $M_{\rm M31} \sim M_{\rm MW}$.

We have omitted the M31 baryonic disc and bulge as well as the fact that its DM halo is elliptical. While the effects of the baryonic disc can be neglected, the effects of the non-spherical DM halo may be significant. Deviation from spherical symmetry of the background potential will contribute to changes of the angular momentum of each satellite. However, we leave this discussion to future work, where we would like to explore this effect in order to place a bound on the ellipticity of the M31 DM halo. Furthermore, our orbit integrator does not include the effects of dynamical friction that a dark matter halo would exert on the satellite. A simple estimate using the Chandrasekhar formula shows that a $10^{10}\ \mathrm{M_\odot}$ satellite galaxy would slow down by about $7\,\mathrm{km\,s^{-1}}$ on an $r = 200$ kpc orbit, but for closer orbits this effect would be more significant. For a review of importance of dynamical friction as a way to distinguish cosmological models with and without dark matter, see Kroupa (2015).

2.4 Uncertainties

We have found that varying the line-of-sight velocities within the uncertainty band in Table 1 does not significantly alter our results, so we do not include the impact of these variations in our work.

On the other hand, the uncertainties in the heliocentric distance measurements to the satellites are much more significant. To include this effect, we evaluate $r_{\rm max}$, $r_{\rm min}$, and $d_{\rm max}$ for five values of distance:

$$\Delta \in \{\Delta_0 + \epsilon_+, \Delta_0 + \epsilon_+/2, \Delta_0, \Delta_0 - \epsilon_-/2, \Delta_0 - \epsilon_-\}, \quad (10)$$

where Δ_0 is the central value of the distance and ϵ_+ and ϵ_- are the upper and lower edges of the 1σ uncertainty band from Table 1.

We have also propagated the uncertainty due to the proper motion of M31. This offset can be treated as constant across the whole range of proper motion we show in our plots. In order to make this systematic uncertainty apparent, we show the M31 PM uncertainty in every plot in Figs 1 and 2 as a green ellipse.

3 CONSTRAINTS

If the plane of satellites is a permanent feature, we expect it to be rotationally stabilized. This implies that the orbits of the in-plane satellites are constrained to be bound, the satellites must be able to survive on their orbits and they do not make large excursions away from the plane.

The first two criteria are not hard to implement: the orbit is bound if the energy of the satellite is negative

$$E < 0. \quad (11)$$

A slightly more stringent condition would be to require that the maximum excursion of the satellite away from M31 is less than the virial radius of M31 (500kpc). Otherwise, the satellite would not be identified as M31's satellite and would eventually cross into the Milky Way gravitational potential. This criterion is then

$$r_{\rm max} < 500\,\mathrm{kpc}, \quad (12)$$

which replaces the previous criterion from equation (11). We would like to note that if a satellite is orbiting in the M31 plane of satellites, it is only a matter of time before its orbit's major axis is pointing at the MW, because orbits in the NFW profile precess fairly rapidly and the M31 plane is nearly edge-on to the MW. As a result, excursions past the virial radius are very likely to result in an eventual loss of the satellite.

If a satellite galaxy comes too close to M31, the tidal interactions strip its content and disrupt the satellite. Therefore, we impose a bound on the satellite's closest approach to M31. In this work, we choose to implement this bound as

$$r_{\rm min} > 15\,\mathrm{kpc}. \quad (13)$$

We can think of this scale as an approximate Roche limit for a satellite of mass of the order of $10^7\ \mathrm{M_\odot}$ of size 0.5 kpc orbiting an enclosed mass of the order of $10^{11}\ \mathrm{M_\odot}$. This is a conservative bound, because in reality such close encounters are still somewhat dangerous.

The third criterion can be implemented in two different ways. We could require that in order to be a permanent member of the plane the angular momentum of the satellite has to be aligned with the normal to the plane. This is equivalent to demanding that the θ from equation (8) is smaller than some reference angle θ_0. The angle θ_0 is related to the scatter of these angles for satellites we consider in-plane. The authors of Pawlowski & Kroupa (2013, 2014) have done just that and have chosen $\theta_0 = 37^\circ$ for the MW plane (the somewhat large size of this angle is driven by the fact that the MW plane is thicker than the M31 plane). We could determine θ_0 from the scatter of the $\boldsymbol{n}$ on the unit sphere and this method will be discussed in upcoming work.

However, even if $\theta < \theta_0$, it is still possible for a satellite to stray far from the plane by a large radial excursion, which would make it appear as a non-member. For this reason, we require that each satellite does not make excursions far away from the plane by requiring that

$$d_{\rm max} < \{1, 2, 3\} \times \sigma_{\rm d} \approx \{13, 25, 37\}\mathrm{kpc}, \quad (14)$$

where $\sigma_{\rm d}$ is defined in equation (4). Another advantage of expressing the third criterion this way is that $\sigma_{\rm d}$ is a directly observable scale and can be determined from the data.

A choice of $(\mu_{\alpha*}, \mu_\delta)$ that satisfies the conditions in equations (12)–(14) leads to an orbit that is consistent with a stable plane composed of the first 15 satellites in Table 1.

4 RESULTS AND DISCUSSION

4.1 Proper motion predictions

We present our results as a phase plot in $\mu_{\alpha*}$ and μ_δ in Figs 1 and 2. The trajectory for each PM is tested against the constraints for five heliocentric distances from the set in equation (10), as discussed in Section 2.4.

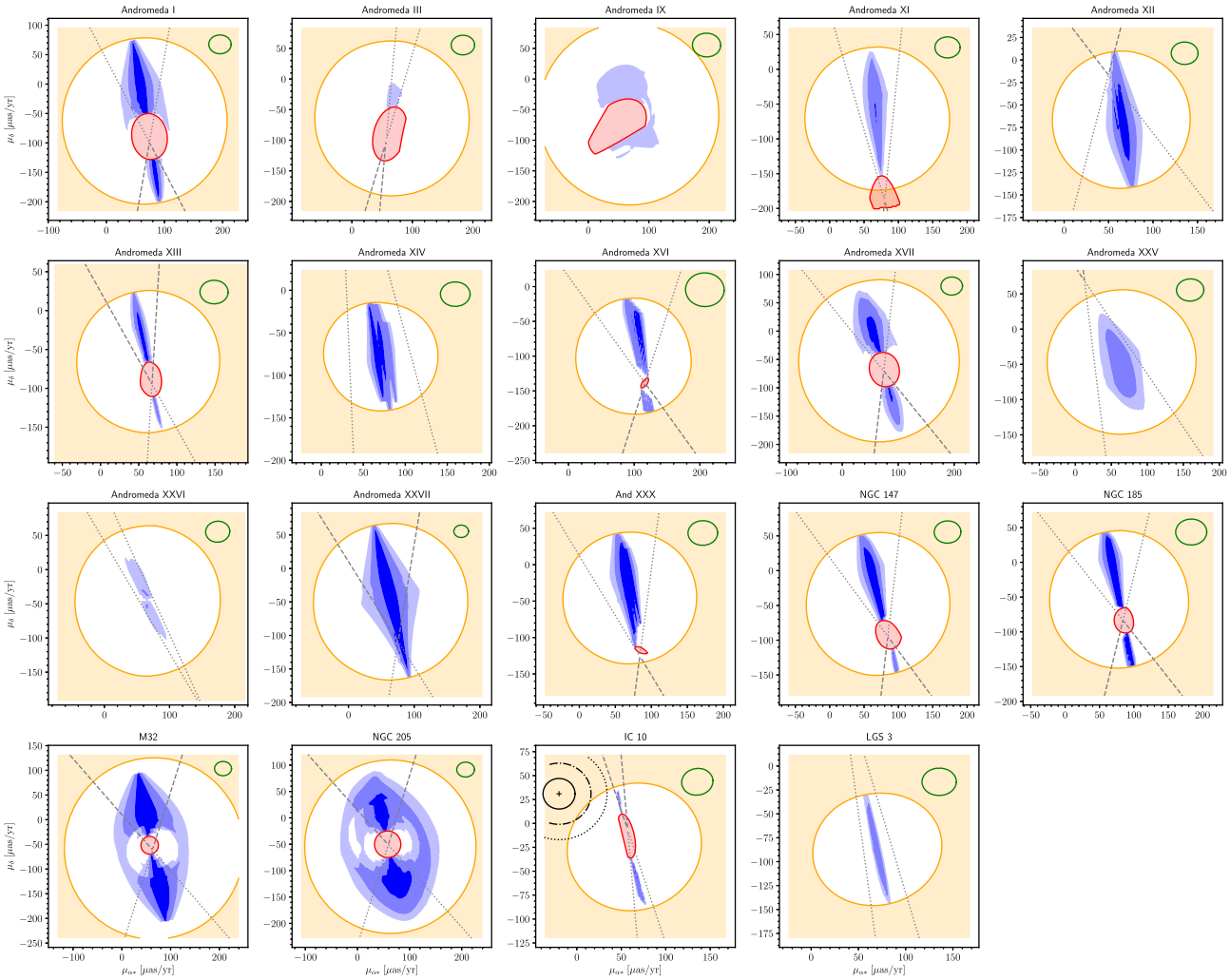

Figure 1. Predicted PMs of satellites of M31. The blue region indicates PMs that are consistent with the satellite staying within $\{1, 2, 3\}\sigma_{\rm D}$ of the plane from darkest to lightest. The red region indicates PMs for which the satellite comes closer than 15 kpc to the centre of the M31 galaxy and is very likely to get disrupted. The orange region indicates PMs for which the satellite wonders off more than 500 kpc from the M31 galaxy. All of the previous regions are marginalized over 1σ band of distance measurements. The grey lines indicate the regions for which the angle between the satellite's angular momentum and the normal to the plane of satellites is less than 30 deg (for the central value of satellite distance). The dotted lines indicate $\boldsymbol{L}$ and $\hat{n}$ are almost aligned, while the dashed lines enclose a region in which they are anti-aligned. Finally, the green circle indicates the uncertainty on the PM of the M31 galaxy itself. The top three rows (first 15 satellites) have been identified by Ibata et al. (2013) as very likely members of the plane. The bottom row (last four satellites) are possible members. The plot for the fifth possible satellite, IC1613, is missing because there are no proper motions that keep IC1613 within 500 kpc of M31. The plot of IC10 also shows the measurement of its proper motion by Brunthaler et al. (2007) and the 1σ, 2σ, and 3σ combined error-ellipsoids are shown as solid black, dash–dotted black, and dotted black.

The coloured regions are defined as follows:

(i) The blue regions contain values of PMs that pass the constraints, and are consistent with the satellite staying within $\sigma_{\rm d}$, $2\sigma_{\rm d}$, and $3\sigma_{\rm d}$ of the plane in at least one distance realization (from darkest to lightest).

(ii) The orange region contains trajectories that stray further than 500 kpc from M31, i.e. which fail condition (12) for all five distance realizations. The boundaries of these regions lie on velocity contours, so the constraint essentially imposes a maximum velocity.

(iii) The red region indicates trajectories that come closer than 15 kpc to the centre of M31, i.e. that fail condition (13) in all five distance realizations. As expected these regions lie around the singularity of the angle contours, corresponding to orbits with small angular momentum.

The uncertainty in the PM of the M31 galaxy itself is indicated by a green circle in each plot, as discussed in Section 2.4.

We include grey dashed lines that indicate the regions for which the angle, θ, between the satellite's angular momentum and the normal to the plane of satellites is less than 30 deg (for the central value of satellite distance). In Pawlowski & Kroupa (2013, 2014) and Pawlowski et al. (2015), MW satellites with $\theta < 37^\circ$ were considered to be co-orbiting within the MW's plane of satellites. This approach produces predictions that are independent of the mass of M31, as a larger M31 mass allows higher velocity orbits along the same angular direction. However, higher velocity orbits can deviate from the plane significantly for even a small value of θ, and the $\theta < 37^\circ$ region on its own fails to include a restriction on such trajectories. For this reason, we believe equation (14), which defines our blue regions, gives a better indication of

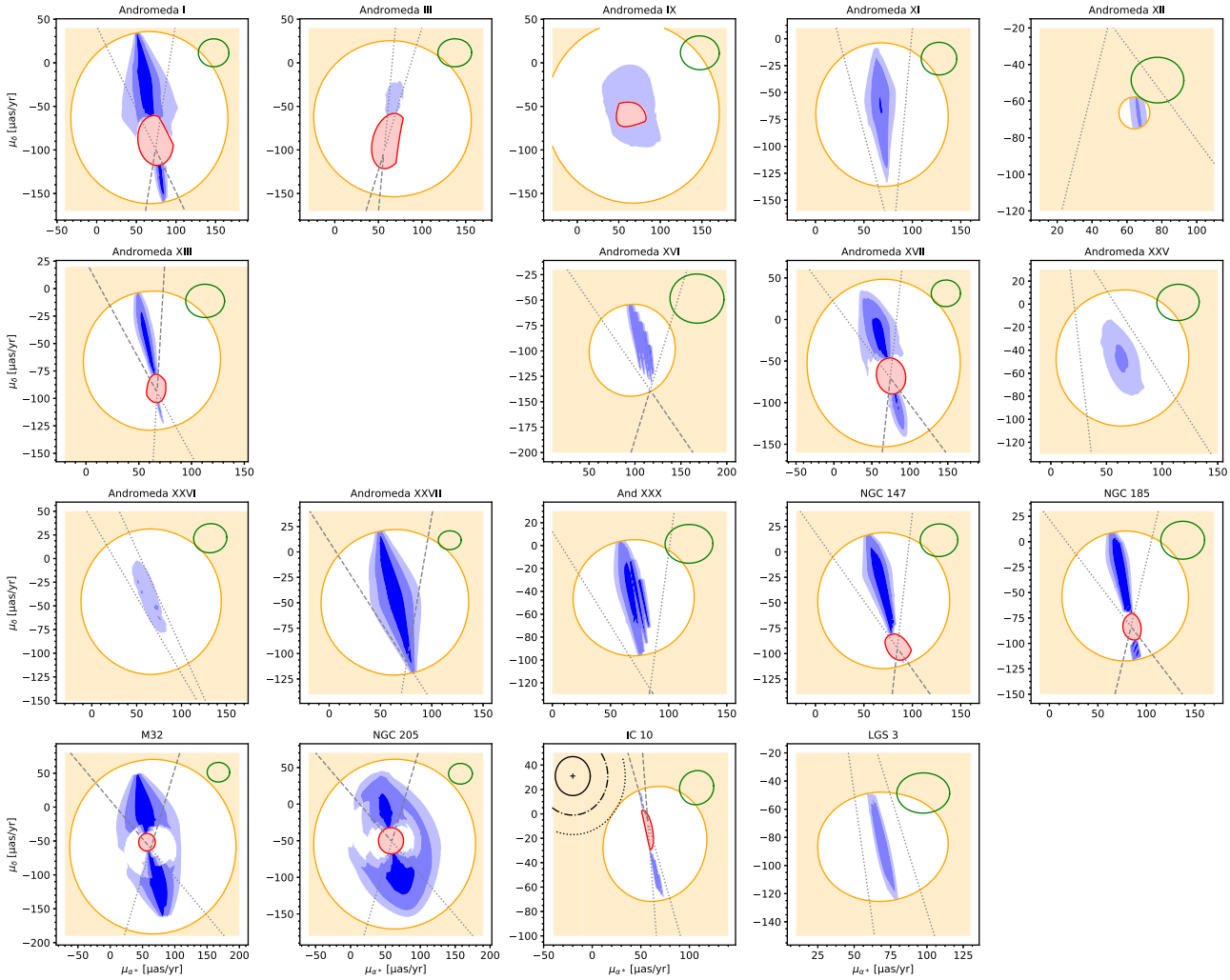

Figure 2. Predicted proper motions of satellites of M31 with the ansatz $M_{\rm M31} = M_{\rm MW}$. The colour scheme is identical to the one used in Fig. 1. The plots for IC 1613 and Andromeda XIV are missing because there are no bound solutions for light $M_{\rm M31}$.

orbits which should truly be considered as stable members of the plane.

The blue regions for most of the satellites are centred on $\theta = 0^\circ$ or 180°, indicating a direction of rotation. The directions of rotation are consistent with those suggested by Ibata et al. (2013), where Andromeda XIII and Andromeda XXVII counter-rotate and the other 13 satellites co-rotate. Our results indicate it may also be possible for Andromeda I and XVII to counter-rotate within the plane, though the counter-rotating regions pass closer than 15 kpc to the centre of M31 for at least one distance realization.

We have also tested every other satellite of M31 (those not considered in-plane by Ibata et al. 2013). None of the other satellites have PMs corresponding to orbits within the plane.

The plots in Figs 1 and 2 can be grouped into three broad categories with similar features:

(i) M32, NGC205, and Andromeda IX are M31's three closest satellites, with distances 23, 42, and 40 kpc from the centre of M31, respectively. As long as their velocity is small enough, there are orbits consistent with the plane for all angles between the satellite's angular momentum and the plane normal. It is likely these satellites are not truly a part of the planar structure, with their position only consistent with the plane due to their close proximity to the origin of M31. Indeed, Ibata et al. (2013) considered M32 and NGC205 as less likely planar members for this reason. The discontinuous nature of the contours in plots for M32 and NGC205 is caused by the fact that the distance uncertainties are significant compared to their actual distance from M31 and hence our five samples from the uncertainty band are not fine enough to produce smooth results. However, given most likely accidental membership in the plane, we feel it is unnecessary to determine the precise nature of these satellites' orbits.

(ii) IC10, LGS3, IC1613, and Andromeda XVI are very far from M31, with distances 252, 269, 520, and 279 kpc, respectively. As a result, only a thin strip of PMs, which correspond to angular momenta very closely aligned to the plane normal, produce trajectories that remain closer than $3\sigma_{\rm D}$ from the plane. IC1613 is so far from the origin of M31 that no PMs correspond to planar orbits, so we do not include it in Figs 1 and 2. Andromeda XVI on the other hand currently lies almost perfectly on the plane, so there is a relatively wide band of PMs consistent with it remaining less than $\sigma_{\rm D}$ from the plane. IC10, LGS 3, and IC1613 are more likely accidentally aligned with the plane.

(iii) Andromeda III, XXV, and XXVI are the furthest offset from the plane of those considered likely to be members by Ibata et al. (2013). As a result the regions consistent with the plane are much smaller (in the Andromeda XXV plot there are no orbits within $1\sigma_d$ of the plane), with too large a velocity or too large an angular momentum deviation from the pane normal resulting in orbits which stray further than $3\sigma_D$ from the plane.

(iv) The remaining satellites were all considered likely members of the plane by Ibata et al. (2013), and have similar spade-like blue regions in Figs 1 and 2. This is due to a relationship between the variable d_{max} in constraint (14) and $\cos\theta$ as defined in equation (8). From the geometry of the setup, it is obvious that $d_{max} \leq \sin(\theta) r_{max}$. However, since the orbits are not closed, over time this inequality is saturated. This explains the shape of the contours: instead of wedges of constant angle, we get shapes that narrow towards larger velocities because larger velocities imply larger r_{max} and hence to keep d_{max} constant, the acceptable range of θ must become smaller.

Finally, we would like to discuss the effect of mass of the host galaxy: the plots in Figs 1 and 2 represent the choices $M_{M31} \sim 2M_{MW}$ and $M_{M31} \sim M_{MW}$. The results are almost identical, up to a rescaling by a factor of $\sim \sqrt{2}$. This is expected because doubling the mass increases the escape velocities by a factor of $\sqrt{2}$. If the line-of-sight velocity is relatively small, then the escape velocity is saturated by the proper motion which results in the size of the orange regions to scale as $M^{1/2}$ as we see. However, if the line-of-sight velocity component is close to saturating the escape velocity alone, then the proper motion components are much more influenced by the change of mass of M31. As an example, the blue regions for Andromeda XII and XIV are more than a factor of $\sqrt{2}$ larger in Fig. 1 compared to Fig. 2. This is because Andromeda XII and XIV have a large velocity relative to M31, at -272 and -208 km s^{-1} (for zero relative proper motion). A larger M31 mass therefore prevents these satellites from making large excursions from M31 and the plane. For the same reason, the red regions in Fig. 1 encroach further on the blue regions, proportionally, than in Fig. 2. This is most noticeable for Andromeda IX and XI.

This brings about an interesting opportunity. When the proper motions of M31's satellites are measured, we can infer a bound on mass of M31 under the assumption that each satellite is a member of a stable plane of satellites.

Similarly, once the proper motions are measured, it is possible to put a constraint on the proper motion of M31, by finding the M31 proper motion that minimizes the d_{max} for all the measured satellites.

4.2 Proper motion of IC10

The existence of a maser in IC10 allowed the authors of Brunthaler et al. (2007) to measure the PM of this dwarf galaxy:

$$\mu_{\alpha*,IC10} = -20 \pm 5\ \mu as\ yr^{-1}$$

$$\mu_{\delta,IC10,exp} = +31 \pm 8\ \mu as\ yr^{-1}.$$

We have shown the value of this measurement in both Figs 1 and 2. The 1σ, 2σ, and 3σ error-ellipsoids are the result of combining the error bars from the PM of M31 and PM of IC10 in quadrature. For heavier M31, Fig. 1, the bound orbit is within 2σ and technically still not ruled out. However, for light M31, all bound orbits with apsis less than 500 kpc are ruled out by 3σ. In both scenarios, all in-plane orbits are ruled out by at least 3σ and therefore it is safe to conclude that the IC10 is unlikely to be a member of the plane.

4.3 Experimental feasibility

Fig. 1 illustrates that in order to distinguish the random alignment hypothesis from the coherent structure hypothesis, it is necessary to measure one of the linear combinations of the PM to accuracy of order 10 μas yr^{-1}. Naturally, we need to ask if this is feasible.

There are two planned measurements by *HST* and *JWST*. The *HST* has already observed the proper motions of NGC147 and NGC 185, with planned accuracy of order 25 km s^{-1}, which corresponds to PMs of order 10 μas yr^{-1} (Sohn et. al., in preparation). The *JWST* has planned guaranteed time observation for the PMs of Andromeda I, III, XIV, and XVII (private communication by van der Marel) with similar planned accuracy. As a result in a couple of years we should have information about 6 out of the 15 members of the M31 plane.

Unfortunately, *GAIA* is unlikely to deliver in this direction. The horizontal branch (HB) in Andromeda I has magnitude around 25 (Costa et al. 1996) in the *V* band. This is similar for most of the M31 satellites as the distance modulus does not vary too much (it is between 23.9 and 24.9 for all the M31 satellites). In the *G* band, this corresponds to magnitude 25.5 for the centre of HB stars.

The *GAIA* satellite has not been directly tested to measure PMs of such dim stars, but naively extrapolating the PM uncertainty relation from Gaia Collaboration (2016) we arrive at an expected measurement uncertainty of order 10^5 μas yr^{-1}. We would need to observe close to 10^8 HB stars in order to determine the PM of Andromeda I to the desired accuracy. Since Andromeda I does not have this many HB stars (or this many stars for that matter), the situation seems hopeless even without dealing with additional caveats associated with our naive extrapolation.

However, the proposed THEIA mission (The Theia Collaboration 2017) has better prospects. With 40 h of observation per satellite over 4 yr, THEIA should be able to achieve PM measurement with uncertainty of order 200 μas yr^{-1} for stars of the 25th magnitude. As a result only a handful of stars (roughly 100) per satellite galaxy would be needed to start resolving the question of stability of the M31 plane. Given that even *JWST* is likely to fly before THEIA is approved, THEIA would only need to observe the remaining nine in-plane satellites. As a result, we would advocate that the THEIA mission would be able to resolve whether or not the M31 plane is a kinematically stable feature with a dedicated total of $\mathcal{O}(400)$ hours of observation.

5 CONCLUSION

We have collected the available data on the three-dimensional position and line-of-sight velocity for 20 of the satellites of M31, 15 of which are believed to form a narrow planar structure. We have calculated the range of possible PMs for each satellite consistent with this plane being a stable structure and the satellite being a member of the structure, by requiring the corresponding orbits to lie close to the plane. The PMs are consistent with the direction of rotation reported in Ibata et al. (2013). Our results consist of predictions of PMs of these satellites and provide a benchmark for future astronomical measurements. We have compared our predictions with previous measurement of the proper motion of IC10 and we conclude it is highly unlikely that IC10 is a proper member of the M31 plane of satellites. Proper motions of other satellites will be published soon (NGC147 and NGC185) and others have been given guaranteed observation time by *JWST* (Andromeda I, III, XIV, and XVII). On top, the proposed THEIA mission (The Theia Collaboration 2017) would be capable of delivering the resolution required to determine whether the true PMs are consistent with the

sets presented here. This would help resolve the question of whether the plane is rotationally stabilized or a temporary structure. If the M31 plane of satellites turns out to be kinematically stabilized, then the tension between ΛCDM and observations will rise, as a result our predictions form a benchmark to test the ΛCDM.

Furthermore, if the measured PMs indicate the plane is at least partially stabilized, we could use the PMs to derive a bound on the mass of M31 and form an independent estimate of the PM of M31 itself.

ACKNOWLEDGEMENTS

We would like to thank Jan Scholtz and Carlos Frenk for fruitful discussions. We would like to thank Marcel Pawlowski for many insights that made this paper much better. We would also like to thank Roeland van der Marel for his help. We would like to thank Steven Abel for support for this project as BH's summer advisor. JS would like to thank the COFUND scheme and the IPPP for his funding. BH would also like to thank the IPPP summer fellowship programme for partial support. We have also benefited from the availability of the ASTROPY software package (Astropy Collaboration 2013; Price-Whelan et al. 2018).

REFERENCES

Astropy Collaboration, 2013, A&A, 558, A33
Brunthaler A., Reid M. J., Falcke H., Henkel C., Menten K. M., 2007, A&A, 462, 101
Buck T., Dutton A. A., Macciò A. V., 2016, MNRAS, 460, 4348
Cautun M., Bose S., Frenk C. S., Guo Q., Han J., Hellwing W. A., Sawala T., Wang W., 2015, MNRAS, 452, 3838
Conn A. R. et al., 2012, ApJ, 758, 11
Costa G. S. D., Armandroff T. E., Caldwell N., Seitzer P., 1996, AJ, 112, 2576
Fritz T. K., Battaglia G., Pawlowski M. S., Kallivayalil N., van der Marel R., Sohn S. T., Brook C., Besla G., 2018, A&A, 619, A103
Gaia Collaboration, 2016, A&A, 595, A1
Gillet N., Ocvirk P., Aubert D., Knebe A., Libeskind N., Yepes G., Gottlöber S., Hoffman Y., 2015, ApJ, 800, 34
Ibata R. A. et al., 2013, Nature, 493, 62
Ibata R. A., Famaey B., Lewis G. F., Ibata N. G., Martin N., 2015, ApJ, 805, 67
Kroupa P., 2015, Can. J. Phys., 93, 169
Kroupa P., Theis C., Boily C. M., 2005, A&A, 431, 517
McConnachie A. W., 2012, AJ, 144, 4
McMillan P. J., 2016, Astrophysics Source Code Library, record ascl:1611.006
McMillan P. J., 2017, MNRAS, 465, 76
Metz M., Kroupa P., Jerjen H., 2007, MNRAS, 374, 1125
Metz M., Kroupa P., Jerjen H., 2009, MNRAS, 394, 2223
Müller O., Pawlowski M. S., Jerjen H., Lelli F., 2018, Science, 359, 534
Pawlowski M. S., 2018, Mod. Phys. Lett. A, 33, 1830004
Pawlowski M. S., Kroupa P., 2013, MNRAS, 435, 2116
Pawlowski M. S., Kroupa P., 2014, ApJ, 790, 74
Pawlowski M. S., McGaugh S. S., Jerjen H., 2015, MNRAS, 453, 1047
Price-Whelan A. M. et al., 2018, AJ, 156, 123
The Theia Collaboration, 2017, preprint (arXiv:1707.01348)
van der Marel R. P., Fardal M. A., Sohn S. T., Patel E., Besla G., del Pino A., Sahlmann J., Watkins L. L., 2019, ApJ, 872, 24
Zentner A. R., Kravtsov A. V., Gnedin O. Y., Klypin A. A., 2005, ApJ, 629, 219

This paper has been typeset from a TEX/LATEX file prepared by the author.